SDC

LONGITUDINAL STUDY OF *RPE65*-ASSOCIATED INHERITED RETINAL DEGENERATIONS

LAURENCE H. M. PIERRACHE, MD, MSc,*†‡§ BABAK GHAFARYASL, MSc,†¶
MUHAMMAD I. KHAN, PhD,**†† SUSANNE YZER, MD, PhD,*
MARIA M. VAN GENDEREN, MD, PhD,‡‡§§ JOSÉ SCHUIL, MD,‡‡ F. NIENKE BOONSTRA, MD,¶¶***
JAN W. R. POTT, MD,††† JAN TJEERD H. N. DE FABER, MD,*
MARTHA J. H. TJON-FO-SANG, MD, PhD,* KOENRAAD A. VERMEER, PhD,†
FRANS P. M. CREMERS, PhD,**†† CAROLINE C. W. KLAVER, MD, PhD,‡§¶¶
L. INGEBORGH VAN DEN BORN, MD, PhD*†

Purpose: To study the disease course of *RPE65*-associated inherited retinal degenerations (IRDs) as a function of the genotype, define a critical age for blindness, and identify potential modifiers.

Methods: Forty-five patients with IRD from 33 families with biallelic *RPE65* mutations, 28 stemming from a genetic isolate. We collected retrospective data from medical charts. Coexisting variants in 108 IRD-associated genes were identified with Molecular Inversion Probe analysis.

Results: Most patients were diagnosed within the first years of life. Daytime visual function ranged from near-normal to blindness in the first four decades and met WHO criteria for blindness for visual acuity and visual field in the fifth decade. p.(Thr368His) was the most common variant (54%). Intrafamilial variability and interfamilial variability in disease severity and progression were observed. Molecular Inversion Probe analysis confirmed all *RPE65* variants and identified one additional variant in *LRAT* and one in *EYS* in two separate patients.

Conclusion: All patients with *RPE65*-associated IRDs developed symptoms within the first year of life. Visual function in childhood and adolescence varied but deteriorated inevitably toward blindness after age 40. In this study, genotype was not predictive of clinical course. The variance in severity of disease could not be explained by double hits in other IRD genes.

RETINA 40:1812–1828, 2020

RPE65-associated inherited retinal degenerations (IRDs) are rare, and they account for 5% to 10% of all autosomal recessive childhood-onset IRDs.[1] Historically, a distinction was made between patients with Leber congenital amaurosis (LCA) and early-onset severe retinal dystrophy (EOSRD) or severe early childhood-onset retinal dystrophy (SECORD). LCA was first described by Theodore Leber[2] in 1869. The obligatory symptoms were congenital amaurosis or highly impaired vision, a large discrepancy between visual function and fundus appearance, an autosomal recessive inheritance pattern, and absent or markedly reduced electrical retinal activity. In 1916, he described a similar disorder with a later onset (6–7 years old) and a milder course of the disease, that was later referred to as EOSRD or SECORD.[3] Nowadays, LCA, EOSRD, and SECORD are considered as part of the same spectrum because of clinical and molecular overlap and account for 5% of all IRDs.[4]

The *RPE65* (retinal pigment epithelium [RPE]-specific protein 65 kDa) gene is exclusively expressed in the RPE, where the protein acts as an isomerase and transforms all-trans-retinyl esters into 11-cis retinol.[5] 11-cis retinol is subsequently converted into 11-cis retinal, which regenerates the visual pigment, chromophore, in photoreceptor cells after light exposure. Without normal functioning RPE65 protein, 11-cis retinal is depleted, and photoreceptor function becomes jeopardized. Rod photoreceptors depend exclusively on 11-cis retinal from the RPE; consequently, an RPE65 protein deficiency leads to severe night blindness from birth.[5] Cone photoreceptors can access 11-cis retinal from an alternative visual pathway taking place in Müller cells.[6] Hence, visual acuity in

daylight remains relatively preserved during childhood. Superimposed on the biochemical dysfunction of the visual cycle, there is a degenerative component, which adds to the development of severe visual impairment. The origin of this degeneration remains unknown, despite increased understanding of the visual cycle.

Multiple therapeutic approaches for *RPE65*-associated IRDs have been evaluated such as pharmacological substitution therapy with oral 9-cis retinal,[7] an artificial chromophore, and gene augmentation therapy[8–11] to bypass the biochemical blockade caused by *RPE65* mutations. Although these therapies have shown to partially reverse the dysfunctional component,[7–11] they have not succeeded to slow or arrest the degenerative process in humans. The limitations of these trials can be attributed to many reasons, but the incorrect timing of administration within the clinical course of the disease may be an important explanation. Preferably, therapeutic interventions are administered before a critical number of photoreceptors are lost because of degeneration[12] and retinal remodeling.[13] Although it is recognized that retinal degeneration in RPE65 starts early in life,[14,15] exact figures from a large group of patients about the clinical course and its determinants such as the *RPE65* genotype and genetic modifiers are scarce,[8,16–37] but are of utmost importance as gene augmentation therapy has been approved by the Food and Drug Administration (FDA) in December 2017 and is becoming available for the *RPE65* population.

We studied data from two cohorts of patients with *RPE65* IRDs: an inbred cohort from a genetic isolate and an outbred cohort with unrelated families from our clinics. This unique combination offers the opportunity to search for genotype–phenotype correlations and to investigate whether subjects with identical *RPE65* variants experience a similar natural course of the disease. We, therefore, performed a longitudinal study in patients from this genetic isolate and unrelated families and studied the natural course of the disease as a function of the *RPE65* genotype and assessed the critical age for development of blindness.

In the genetic isolate, we have also come across patients with IRDs caused by variants in other IRD-associated genes such as *LRAT*, *FAM161A*, and *USH2A*. Using recently developed Molecular Inversion Probes (MIPs) technique, we also examined 108 other IRD genes to identify potential modifiers of RPE65-mediated IRDs. Especially genes that are part of the visual cycle (*ABCA4*, *LRAT*, *RDH12*, and *RLBP1*) were of interest.

Methods

Subjects

In 1959, Schappert-Kimmijser et al described an isolated population living in the northwest of the Netherlands with a relatively high prevalence of LCA. In 2003 Yzer et al[38] discovered a founder mutation in the *RPE65* gene (p.Tyr368His) in 14 patients from this genetic isolate. For this study, we gathered longitudinal data from these original 14 patients (Table 1). We included 14 more patients from the same genetic isolate and 16 patients with *RPE65*-associated IRDs from our ophthalmogenetic outpatient clinics in Rotterdam. Finally, we queried our partners of the RD5000 consortium,[39] resulting in a cohort of 45 patients from 33 families with *RPE65*-associated IRDs.

Medical records were reviewed to extract medical history, family history, molecular diagnosis, and longitudinal visual function testing. Fifteen patients were invited for a complete ophthalmic examination with visual function assessment and fundus imaging because they had not been evaluated in the past 5 years. Prospective clinical data from another 17 patients were gathered during the period of this study (January 1st, 2014–April 30th, 2017) as part of routine follow-up. Best-corrected visual acuity (BCVA) was measured in preschool children with Lea symbols[40] or E charts. In literate patients, Early Treatment Diabetic Retinopathy Study (ETDRS) or Snellen charts were used. All BCVA

From the *The Rotterdam Eye Hospital, Rotterdam, the Netherlands; †Rotterdam Ophthalmic Institute, Rotterdam, the Netherlands; ‡Department of Ophthalmology, Erasmus Medical Center, Rotterdam, the Netherlands; §Department of Epidemiology, Erasmus Medical Center, Rotterdam, the Netherlands; ¶Department of Imaging Physics, Delft University of Technology, Delft, the Netherlands; **Department of Human Genetics, Radboud University Medical Center, Nijmegen, the Netherlands; ††Department of Cognitive Neuroscience, Radboud University Medical Centre Nijmegen, Donders Institute for Brain, Cognition and Behaviour, Nijmegen, the Netherlands; ‡‡Bartiméus Diagnostic Centre for Complex Visual Disorders, Zeist, the Netherlands; §§Department of Ophthalmology, University Medical Centre Utrecht, Utrecht, the Netherlands; ¶¶Department of Ophthalmology, Radboud University Medical Center, Nijmegen, the Netherlands; ***Royal Dutch Visio, National Foundation for the Visually Impaired and Blind, Huizen, the Netherlands; and †††Department of Ophthalmology, University Medical Center Groningen, Groningen, the Netherlands.

Supported by Combined Ophthalmic Research Rotterdam (CORR) grant.

Presented in part at the Association for Research in Vision and Ophthalmology, Seattle, WA, May 1, 2016.

None of the authors has any conflicting interests to disclose.

Supplemental digital content is available for this article. Direct URL citations appear in the printed text and are provided in the HTML and PDF versions of this article on the journal's Web site (www.retinajournal.com).

Reprint requests: L. Ingeborgh van den Born, MD, PhD, The Rotterdam Eye Hospital, Schiedamse Vest 180, 3011 BH Rotterdam, the Netherlands; e-mail: born@eyehospital.nl

Table 1. Demographic and Genetic Characteristics of Patients Included in this Study

ID	Gender	Age Last Visit	Follow-up (years)	DNA Variation	Protein Variation	DNA Variation	Protein Variation	MIPs Variant
A1*	M	20	17	c.1102T>C	p.(Tyr368His)	c.1102T>C	p.(Tyr368His)	
B1*	M	37	37	c.1102T>C	p.(Tyr368His)	c.1102T>C	p.(Tyr368His)	
B2*	M	38	7	c.1102T>C	p.(Tyr368His)	c.1102T>C	p.(Tyr368His)	
C1*	M	43	38	c.1102T>C	p.(Tyr368His)	c.1102T>C	p.(Tyr368His)	
D1*,[8]	M	26	18	c.1102T>C	p.(Tyr368His)	c.1102T>C	p.(Tyr368His)	
E1*	M	34	29	c.715T>G	p.(Tyr239Asp)	c.715T>G	p.(Tyr239Asp)	
F1*	M	18	18	c.1102T>C	p.(Tyr368His)	c.1102T>C	p.(Tyr368His)	
G1	M	27	20	c.989 G>A	p.(Cys330Thr)	c.989 G>A	p.(Cys330Thr)	
H1[42]	M	7	4	c.138delG	p.(Pro47Glnfs*47)	c.138delG	p.(Pro47Glnfs*47)	
H2[42]	F	8	6	c.138delG	p.(Pro47Glnfs*47)	c.138delG	p.(Pro47Glnfs*47)	
I1	F	24	9	c.715T>G	p.(Tyr239Asp)	c.715T>G	p.(Tyr239Asp)	
J1*,[8]	M	10	8	c.1102T>C	p.(Tyr368His)	c.11+5 G>A	p.(?)	
K1*	F	7	3	c.1102T>C	p.(Tyr368His)	c.1102T>C	p.(Tyr368His)	*EYS*:c.1673 G>A; p.(Trp558*)
K2*	F	10	8	c.1102T>C	p.(Tyr368His)	c.1102T>C	p.(Tyr368His)	*EYS*:c.1673 G>A; p.(Trp558*)
L1*,[8]	F	12	0	c.11+5 G>A	p.(?)	c.11+5 G>A	p.(?)	
M1[42]	M	27	7	c.1102T>C	p.(Tyr368His)	c.208T>G	p.(Phe70Val)	
N1	F	41	0	c.271C>T	p.(Arg91Trp)	c.715T>G	p.(Tyr239Asp)	
O1*	M	24	22	c.1102T>C	p.(Tyr368His)	c.1102T>C	p.(Tyr368His)	
O2*	F	33	27	c.1102T>C	p.(Tyr368His)	c.1102T>C	p.(Tyr368His)	
O3*,[25]	M	34	31	c.1102T>C	p.(Tyr368His)	c.1102T>C	p.(Tyr368His)	*LRAT*:c.12del; p.(Met5Cysfs*54)
P1	F	48	32	c.1102T>C	p.(Tyr368His)	c.361del	p.(Serf121 fs)	
Q1	M	29	9	c.859 G>T	p.(Val287Phe)	c.859 G>T	p.(Val287Phe)	
R1*	M	15	13	c.1102T>C	p.(Tyr368His)	c.11+5 G>A	p.(?)	
S1*,[8]	M	20	18	c.1102T>C	p.(Tyr368His)	c.1102T>C	p.(Tyr368His)	
T1*	F	5	3	c.1102T>C	p.(Tyr368His)	c.1102T>C	p.(Tyr368His)	
T2*	F	0	NA	c.1102T>C	p.(Tyr368His)	c.1102T>C	p.(Tyr368His)	
U1*	F	29	24	c.1102T>C	p.(Tyr368His)	c.1102T>C	p.(Tyr368His)	
V1*	M	30	24	c.1102T>C	p.(Tyr368His)	c.1102T>C	p.(Tyr368His)	
V2*	F	35	21	c.1102T>C	p.(Tyr368His)	c.1102T>C	p.(Tyr368His)	
V3*	M	31	23	c.1102T>C	p.(Tyr368His)	c.1102T>C	p.(Tyr368His)	
W1*	F	14	7	c.1102T>C	p.(Tyr368His)	c.11+5 G>A	p.(?)	
X1	M	38	15	c.271C>T	p.(Arg91Trp)	c.1067dup	p.(Asn356Lysfs*9)	
X2	F	53	32	c.271C>T	p.(Arg91Trp)	c.1067dup	p.(Asn356Lysfs*9)	
Y1	M	18	NA	c.271C>T	p.(Arg91Trp)	c.271C>T	p.(Arg91Trp)	
Y2	F	7	4	c.271C>T	p.(Arg91Trp)	c.271C>T	p.(Arg91Trp)	
Y3	M	19	15	c.271C>T	p.(Arg91Trp)	c.271C>T	p.(Arg91Trp)	
Z1	F	20	16	c.1102T>C	p.(Tyr368His)	c.1543C>T	p.(Arg515Trp)	
AA1	M	33	29	c.11+5 G>A	p.(?)	c.499 G>T	p.(Asp167Tyr)	
AB1*	M	30	20	c.11+5 G>A	p.(?)	c.11+5 G>A	p.(?)	
AB2*	M	32	7	c.11+5 G>A	p.(?)	c.11+5 G>A	p.(?)	
AC1	F	27	9	c.1102T>C	p.(Tyr368His)	c.1102T>C	p.(Tyr368His)	
AD1	M	8	1	c.715T>G	p.(Tyr239Asp)	c.715T>G	p.(Tyr239Asp)	
AE1*	M	16	14	c.1102T>C	p.(Tyr368His)	c.991-993dup	p.(Trp331dup)	
AF1*	F	9	4	c.1102T>C	p.(Tyr368His)	c.1102T>C	p.(Tyr368His)	
AG1*	M	17	15	c.1102T>C	p.(Tyr368His)	c.1102T>C	p.(Tyr368His)	

*Stems from genetic isolate; MIPs, Molecular Inversion Probes.

measurements were converted to Snellen visual acuity. Low vision measurements were converted to logarithm of the minimum angle of resolution (LogMAR) visual acuity to enable graphic representation (counting fingers: 2.0, hand movements: 2.3,[41] light perception 2.5, and no light perception 2.6). Patients underwent Goldmann kinetic visual field (VF) testing, full-field electroretinography according to International Society for Clinical Electrophysiology (ISCEV) protocol, and color fundus photography (Topcon Great Britain Ltd, Berkshire, United Kingdom). Spectral domain optical coherence tomography (SD-OCT) and fundus autofluorescence (FAF) (Spectralis; Heidelberg Engineering Ltd, Heidelberg, Germany) were performed in subjects if fixation was possible. The median follow-up was 16 years and ranged from a single visit to 38 years. A subset of patients received gene augmentation therapy (7 patients)[8,42] or pharmacological substitution therapy (1 patient) with synthetic 9-cis-retinyl acetate[25] (Table 1). We have excluded all post-treatment measurements of both eyes of these patients from analysis. Visual impairment was defined as either low vision (BCVA worse than 20/60 but equal or better than 20/400 and/or central VF diameter of the V4e target smaller than 20° but equal or larger than 10° in the better eye) or blindness (BCVA worse than 20/400 and/or central VF diameter of the V4e target smaller than 10° in the better eye) in accordance with the WHO criteria.

Retinal Structure

Cross-sectional images along the horizontal meridian of the central retina were obtained with commercially available SD-OCT instruments (Spectralis, Heidelberg Engineering) using a 20° single line scan crossing the fovea. Spectral domain OCT examination proved very difficult because most patients had nystagmus or nystagmoid movements and could not fixate on the internal target. For qualitative analysis, the best-quality images were selected for each patient, and for quantitative analysis, images were analyzed if manual segmentation was achievable for at least two layers of interest. We quantified thickness of the ganglion cell layer (GCL), the outer nuclear layer (ONL), the photoreceptor–RPE complex, and the total retina in 23 scans from 10 patients with *RPE65*-mediated IRDs (median age: 17 years, range: 4–35 years). A normal data set for the thickness of all four layers on SD-OCT was obtained from 110 eyes from 56 controls (median age: 30 years, range 5–77 years) without retinal or vitreoretinal disease. The GCL was measured from the retinal nerve fiber layer to the inner plexiform layer; the ONL was measured from the outer plexiform layer to the external limiting membrane (ELM); the photoreceptor complex thickness was measured from the ELM to the RPE, and the total retinal thickness was measured from vitreous–retinal interface to the Bruch membrane complex. The reference layers were segmented manually by the same operator (L.H.M.P.) using the thickness graphs in Heidelberg Eye Explorer software (Heidelberg Engineering). To calculate the thickness of the whole retina, ONL, GCL, and photoreceptor–RPE complex as a function of distance to the macula, points were placed on the segmented Bruch membrane at equidistance locations using Matlab (Version 2013b, The MathWorks). Subsequently, at each point, a line perpendicular to the Bruch membrane was obtained. The distance between the intersection of this line and the segmented interfaces that delineate the layer of interest was used to calculate the thickness information, which was normalized for the left and right eyes. In addition, the distance along the Bruch membrane was reported relative to the location of the macula. At each point, the 95% confidence interval and 95% percentile were calculated from the normal data set. Differences in mean thickness of retinal layers were analyzed in cases and controls with a Mann–Whitney *U* test, both in children and adults.

Molecular Diagnosis

The molecular diagnosis was made in 30 patients using PCR amplification and subsequent Sanger sequencing of the *RPE65* gene. In 12 patients, mutations were found using an arrayed primer extension (APEX) microarray chip for LCA (Asper Biotech, Tartu, Estonia) and in two patients using an APEX microarray chip for autosomal recessive retinitis pigmentosa (Asper Biotech). In one patient, targeted analysis of 256 IRD-associated genes after exome sequencing was performed.

Molecular Inversion Probes

An additional genetic analysis was performed in 35 subjects using MIP to sequence 108 IRD-associated genes (see **Table 1, Supplemental Digital Content 1**, http://links.lww.com/IAE/B126). These 108 genes represented all published nonsyndromic IRD-associated genes known in October 2013. Variants were identified and filtered by quality (>200× depth), by allele frequency in gnomAD (<0.005) and by gene component (exon, canonical splice sites, splice site acceptor, splice site donor, and intron).

The study adhered to the tenets of the Declaration of Helsinki, and all procedures were reviewed by the Medical Ethics Committee of Erasmus Medical Center. Patients or patients' guardian provided a written

informed consent to retrieve data from medical records and analyze retrospective and prospectively acquired molecular and clinical data.

Results

Disease Onset and Diagnosis

We studied a cohort of 45 patients with *RPE65*-associated retinal dystrophy, 28 (62%) stem from a genetic isolate in the north of the Netherlands. Patients were grouped per family in Table 1. Most patients were diagnosed with *RPE65*-associated IRD within the first year of life. Parents reported the presence of nystagmus, lack of eye contact, night blindness, or photoattraction. In one patient, low vision was attributed to high myopia, and the correct diagnosis was made at age 17. For three non-Dutch subjects, information on the onset of disease was missing because we could not retrieve historical data from their country of origin. Nystagmus was observed in 33 patients, in nine patients, it was absent, and in three patients, information on nystagmus was lacking. The clinical diagnosis was confirmed by severely reduced or nonrecordable electroretinographic responses (Table 2) and DNA testing (Table 1). There were no patients with late-onset retinal disease caused by *RPE65* mutations in our ophthalmogenetic clinic.

Table 2. Patient Characteristics (N = 45)

Median current age (years)	28 (range 2–59 years)
Sex, no. males (%)	27 (60%)
Ethnicity	
European, no. (%)	37 (81%)
African, no. (%)	5 (12%)
Asian, no. (%)	3 (7%)
Mean age at onset of symptoms (years)	<1 (range 0–3)
Mean age at diagnosis (years)	<1 (range 0–17*)
Refractive error, spherical equivalent (D)	−1.75 (range −11.75 to +5.75)
Mean follow-up time (years)	16 (range 0–38)
Electroretinogram	
Median age (years)	1 (range 0–10)
Rods and cones nonrecordable, no. (%)	31 (86%)
Rods nonrecordable, severely reduced cone response, no. (%)	5 (14%)

*One patient was incorrectly diagnosed as low vision associated with high myopia as a child, and the correct diagnosis was made at age 17.

Fundus Features

Fourteen patients were evaluated by one of the authors during the first year of life and 18 in early childhood (before the age of 5 years). In seven patients (22%), no abnormalities were noted at first visit. A relative dark aspect of the RPE or RPE alterations was observed in the macula in 13 patients, the fovea was hypopigmented (Figure 1A) in one patient, and the foveal reflex was absent in seven patients. Fourteen patients had narrow blood vessels. Three patients (9%) had hypopigmented, blond fundi, and nine patients (28%) had subtle RPE changes in the periphery. In four children, white dots were apparent early in life, but these disappeared with aging (Figure 2). Intraretinal pigment migration and atrophy of the RPE only became apparent in the second decade of life and was first recorded at the age of 13 years. In 15 patients, no intraretinal hyperpigmentations were seen at last visit (median age: 8 years, range: 0–20 years).

Quantitative and Qualitative Analysis of Spectral Domain Optical Coherence Tomography Images

The mean total retinal thickness was reduced in scans from children (n = 12) between the ages of 5 and 19 years, compared with controls (n = 26) ($P = 0.000002$) (Figure 3). The mean thickness of the GCL was comparable in patients and controls ($P = 0.45$), whereas the mean thickness of the ONL ($P = 0.000001$) and the outer retinal layers ($P = 0.000001$) was significantly reduced in patients. The retinal lamellar architecture was mostly well preserved; however, a better preservation did not seem to be associated with a better visual function (Figure 4). Patients K1, W1, and AE1 (Figure 4, A–C) had an intact photoreceptor layer with a continuous ELM and ellipsoid zone (EZ), but their visual acuity was poor (hand movements) compared with patients within the same age category (at 4, 10, and 11 years of age). The EZ in these patients appeared less intense than in controls, but there were no gross abnormalities visible. A single patient, Y2 (Figure 4D), showed signs of central retinal degeneration at 8 years old; the ELM was only discernible in the perifoveal region but not in the fovea, and the EZ appeared to be absent in the macular region.

In adults, the mean total retinal thickness was reduced in patients (n = 8) compared with controls (n = 78) ($P = 0.002$) (Figure 3). The GCL thickness was comparable in patients and controls ($P = 0.08$). As in children, the mean thickness of the ONL ($P = 0.000009$) and outer retinal layers ($P = 0.0002$) was significantly reduced. A small subset of patients had

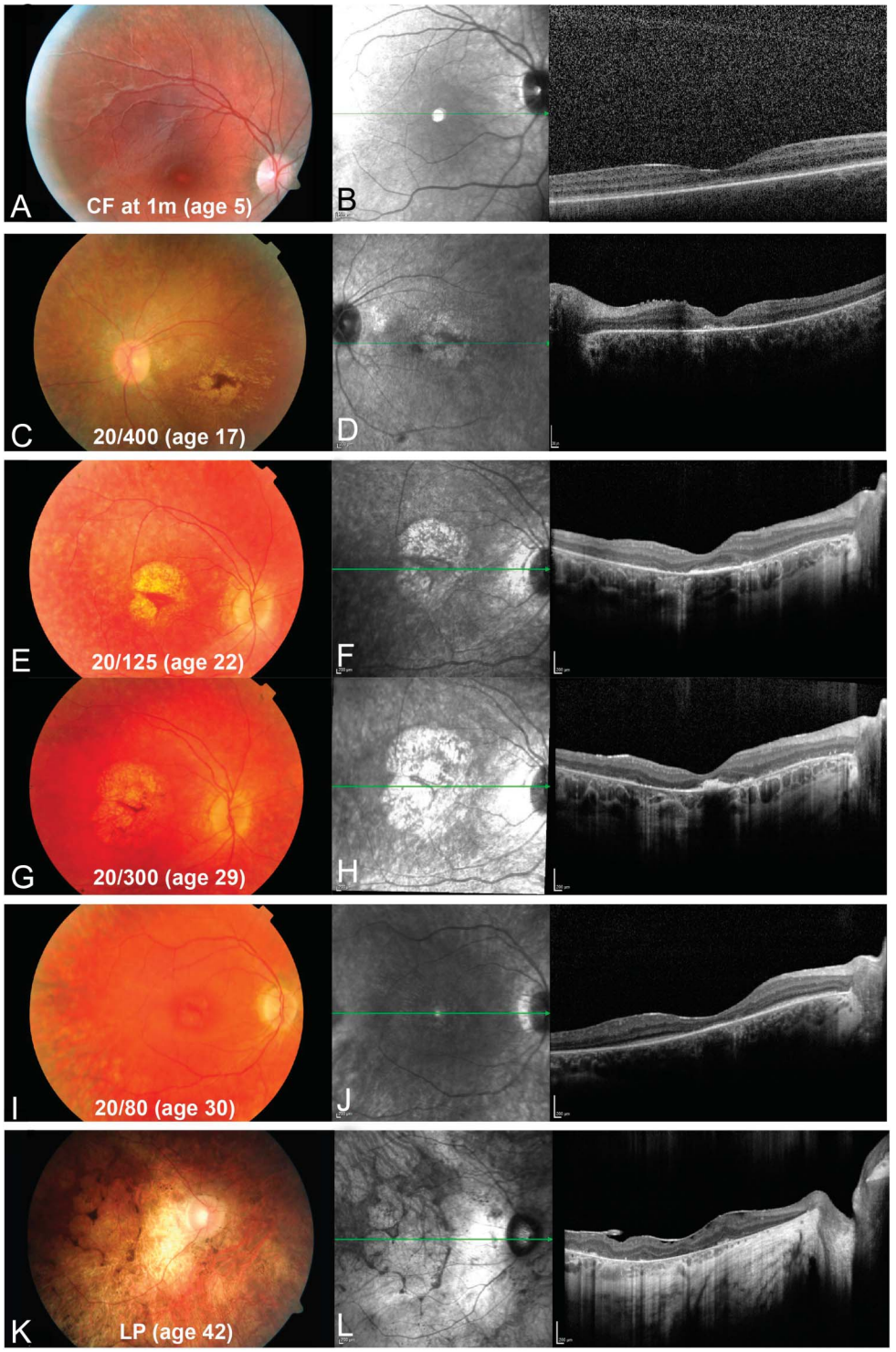

Fig. 1. Macular abnormalities in patients with *RPE65*-mediated IRDs. Fundus images, infrared images, and SD-OCT. Patient T1, (**A**) the fovea appears hypopigmented, whereas the pigmentation in the periphery is coarse, (**B**) the outer retinal layers appear to be continuous over the length of the retinal scan, and the ELM is hard to distinguish and might be absent. Patient Z1, (**C**) revealing a small remaining hyperpigmented foveal island, (**D**) the outer retina is disrupted with central hyperreflective remnants. Follow-up imaging of patient U1 at age 22 (**E** and **F**), and 7 years later (**G** and **H**). On scan (**E**), the outer retina is disrupted with hyperreflective foveal lines visible, possibly there is some remaining ELM, ellipsoid, and/or interdigitation zone. On the follow-up scan (**F**), there is atrophy the outer retina, a subfoveal hyperreflective deposit with nasally possible ELM remnants. Patient AA1 (**I** and **J**), imaging reveals absent outer retina with exception of subfoveal and small parafoveal areas with some sparing of the ellipsoid/interdigitation zone but absent ELM. Patient B1 (**K**) with end-stage disease, (**L**) RPE and Bruch membrane are intact, the outer retina is completely absent with some hyperreflective deposits on the RPE that correspond to hyperpigmentation. There is also an epiretinal membrane present.

a relatively well-preserved central retinal architecture in their twenties, with both the ELM and EZ clearly distinguishable in the foveal region (Figure 4, E–H). Patients with preserved architecture had a better visual function. Thirteen patients developed pronounced atrophy of the RPE and photoreceptor layers in the macula, as early as the age of 17 years. The atrophy started in the perifoveal region and crept up to the center of the fovea (Figure 1), causing severe visual impairment.

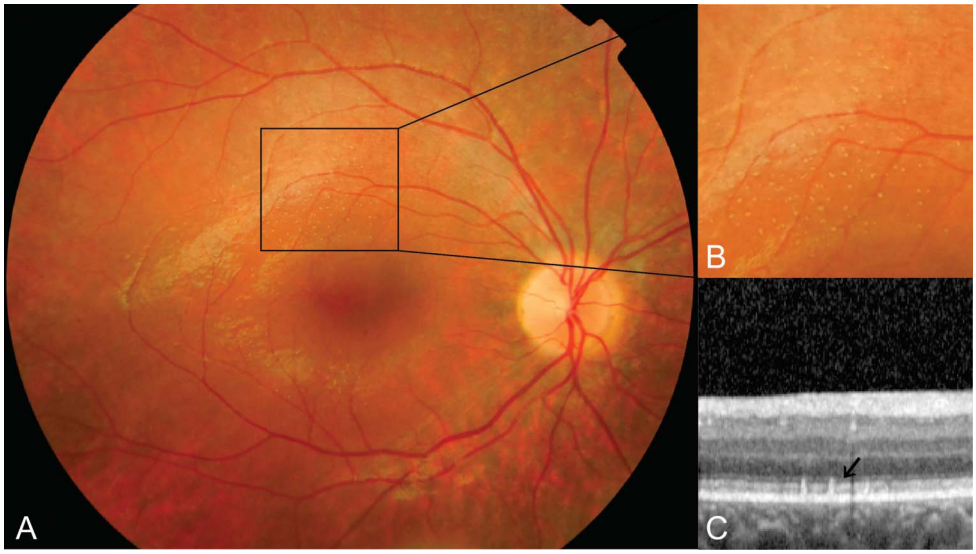

Fig. 2. Retinal imaging of white dots in a patient with *RPE65*-mediated IRDs. Fundus photograph (**A** and **B**) and OCT scan (**C**) of patient W1 aged 10 years, showing white sharp demarcated dots at the level of the RPE and outer segment. Black arrow indicates the white deposits.

Fundus Autofluorescence

In most patients, it was not possible to obtain good-quality FAF images, due to absence of autofluorescence, poor fixation, and a photophobic reaction to blue light. In 17 patients, FAF imaging was not performed, and in 22 patients, the quality of the image was too low for interpretation. In eight eyes from six patients, we were able to produce images (Figure 5), but with a bright appearance of the optic disk, indicating inaccurate sensitivity settings during acquisition; therefore, care must be taken with interpretation. In four patients, a hyperautofluorescent ring was visible in the posterior pole. The diameter of this ring ranged from the parafoveal area to encompass the entire posterior pole (Figure 5, C–F).

Visual Function

The follow-up period was left-skewed because our cohort was relatively young; the median age was 28 years (Table 2). Best-corrected visual acuity measurements were available for 43 of 45 subjects; in one subject, it was impossible to record reliable measurements because of young age (<1 year) and in one subject because of intellectual disability. The median follow-up of visual acuity was 15 years (Table 1). There was no correlation between visual acuity and the presence of nystagmus. Nine patients had high myopia (more than −6.00 D), and eight patients had moderate myopia (between −3.00 D and −6.00 D). The median refractive error was −1.75 D. In five patients, we measured a significant difference in visual acuity between both eyes, greater than the test–retest variability of four lines (0.3 LogMAR), at two or more consecutive measurements (Figure 6B). They were diagnosed with amblyopia in the past in presence of amblyogenic risk factors such as anisometropia, uncorrected refractive error, or strabismus. Treatment of the underlying cause (e.g., correction of refractive error, patching, or strabismus surgery) could not improve visual acuity of the amblyopic eye. In other patients, the decreased visual acuity was symmetric.

The course of visual acuity for the best-performing eye as a function of age is shown in Figures 6 and 7. The variability in visual acuity between subjects is large in the first decade of life, ranging from 20/20 to counting fingers at 1 meter. However, visual acuity remained stable in childhood and early adulthood, both in the best- and worst-performing eye, but inevitably progresses toward blindness in the 5th decade of life (Figures 6 and 7). In a subset of patients, this was the result of pronounced atrophy of the fovea (Figure 1).

Kinetic VFs were available for 33 subjects and were graded according to the WHO criteria for low vision and blindness. In childhood, VFs reached beyond 20° radius for the V4 target, but with increasing age, the radius of the central VF decreased. At age 28, 50% of patients met the criteria for low vision and at age 38 for blindness (Figure 7).

Electroretinography

Electroretinograms (ERGs) were performed at diagnosis and were not routinely repeated during follow-up. Thirty-one patients had no detectable ERGs to any stimuli, and five patients showed severely reduced cone responses with extinguished rod responses. Because we depended on retrospective data for ERG

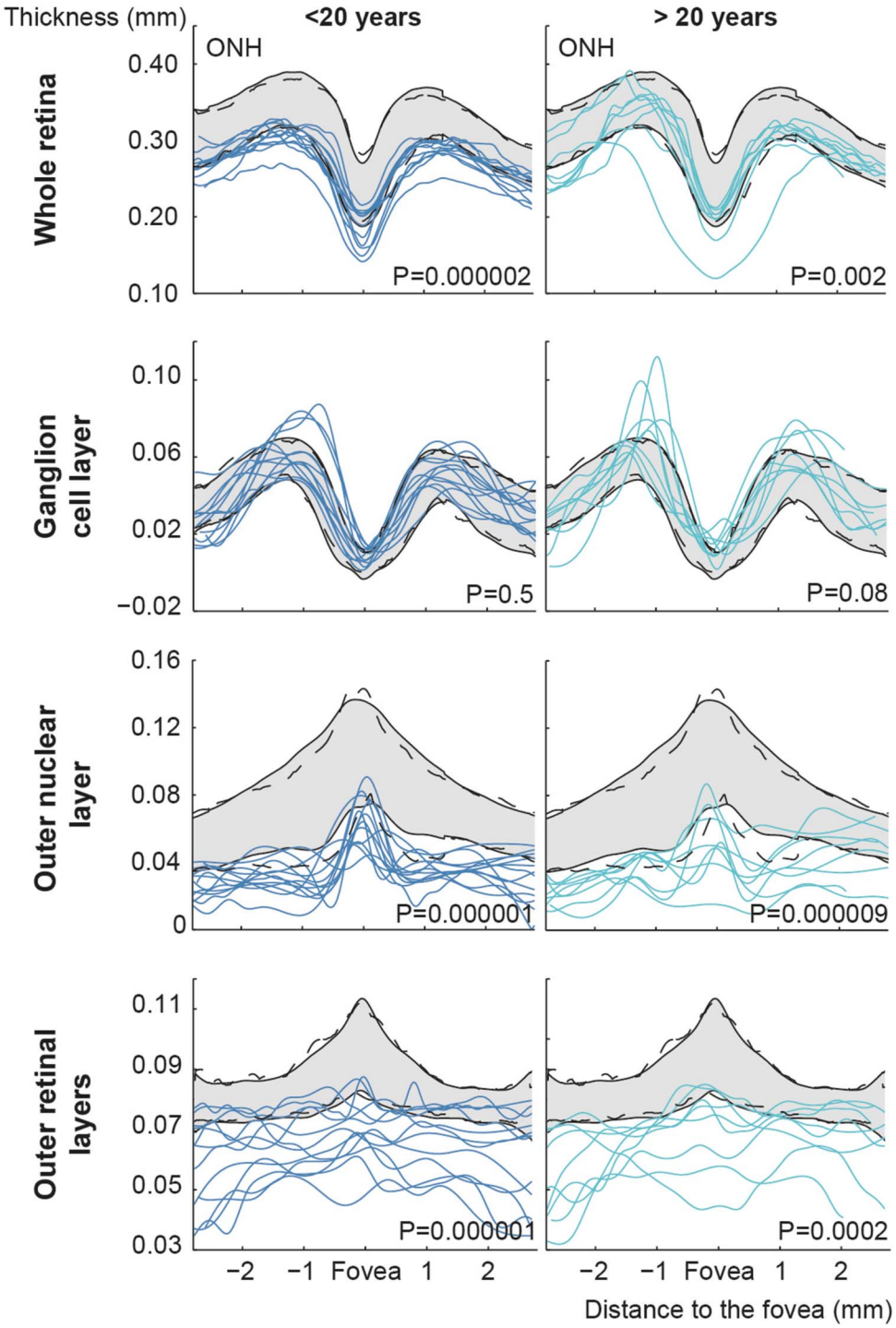

Fig. 3. Thickness of retinal layers. Thickness measurements of the total retina, GCL, ONL, and outer retinal layer in 20 scans from 10 patients with *RPE65*-mediated IRDs. The gray band represents the 95% confidence interval, the dashed lines represent the 2.5th and 97.5th percentiles, and each colored line represents a single line scan. ONH, optic nerve head.

testing from different centers, we could not compare amplitude values or latency values.

Molecular Genetics

Biallelic variants in *RPE65* are summarized in Table 1, and additional information on previously reported isomerase activity, in silico functional analyses, and allele frequencies in healthy persons is listed in Table 3. We found eight missense variants, three frameshift variants, one intronic variant, and one splice site variant. Three missense variants were previously tested in vitro and were considered nonhypomorphic, as their isomerase activity fell below 10% of the wildtype

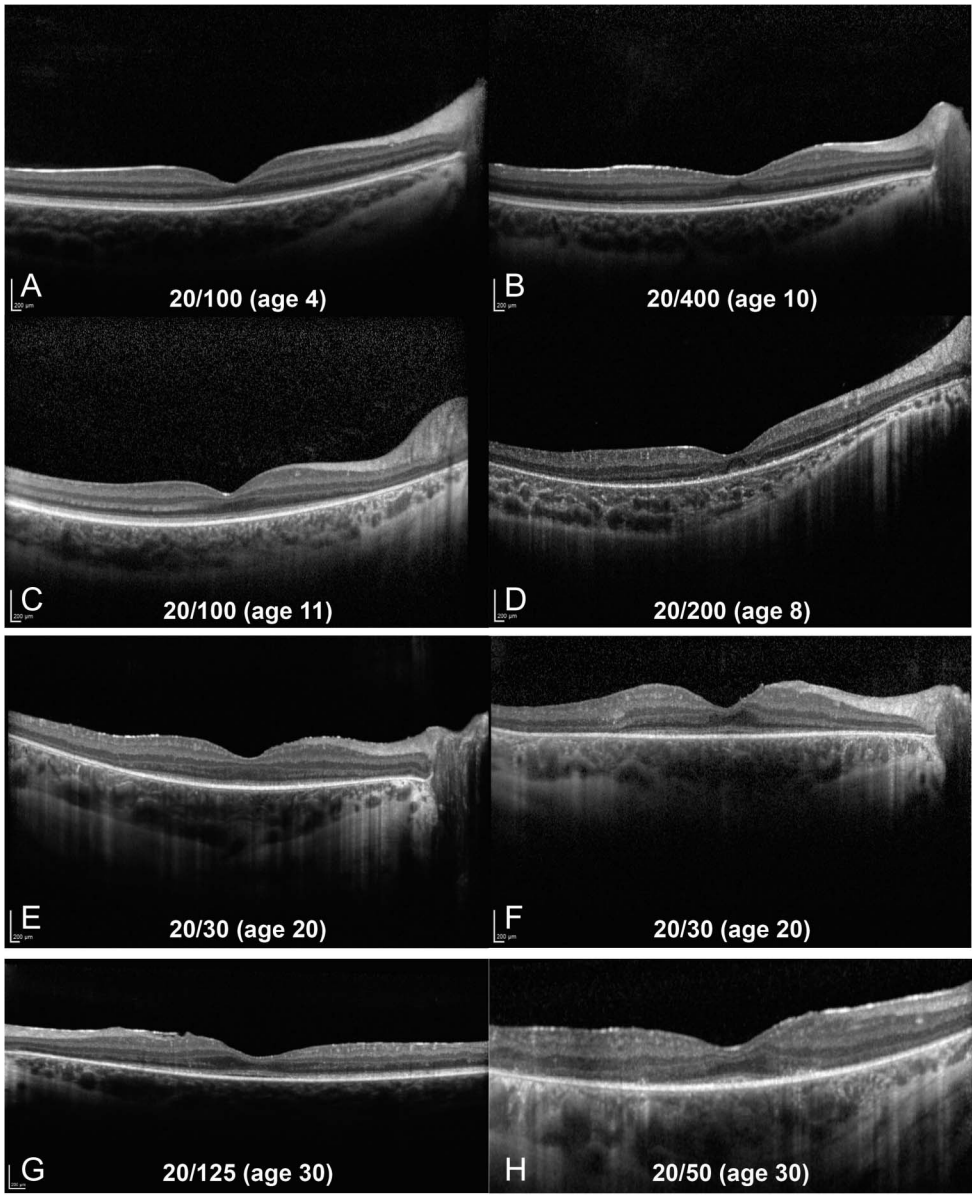

Fig. 4. Spectral domain OCT scans in patients with *RPE65*-mediated IRDs. Spectral domain OCT scans showing preservation of the lamellar architecture of the retina in patient K1 (**A**) and patient W1 (**B**) appears, with a normal ELM. In patient AE1 (**C**), the outer retina appears normal in the center, but toward the optic nerve, there is atrophy. The ONL appears thinner than in normal subjects, the ELM and EZ are continuous, and the foveal bulge is present. The EZ appears less intense, compared with healthy controls in **A**, **B** and **C**. Spectral domain OCT of patient Y2 (**D**) shows a disruption of the subfoveal and atrophy of the parafoveal outer retina, with subfoveal and extrafoveal remnants of the outer retina but hard to distinguish between ELM/ellipsoid or interdigitation zone. These remnants are lost toward more peripheral areas. Imaging in patient F1 (**E**), patient M1 (**F**), patient AB1 (**G**), and patient 01 (**H**) reveals a well-preserved central retinal architecture, with both the ELM, interdigitation zone, and EZ clearly distinguishable in the center and parafoveal atrophy of these outer layers in various degrees.

protein.[43,44] Twenty-one patients were homozygous for p.(Thr368His), and seven patients were heterozygous carriers, making it the most common variant in our cohort (54%). This founder mutation was found in eight of the 121,144 alleles (0.007%) in ExAC, but exclusively in subjects of European descent. In addition, we found this variant in two of 3,184 alleles from whole-exome sequencing data from a Dutch outbred cohort, the Rotterdam Study (0.04%).[45]

Molecular Inversion Probe testing in 35 patients picked up all *RPE65* variants that were previously identified as causal by other DNA analysis techniques (see Table 1, **Supplemental digital content 2,** http://links.lww.com/IAE/B127). In 25 patients (71%), no variants in other IRD-associated genes were identified after filtering. In 10 patients, eight different variants were detected, of which two were classified as benign (*MERTK* and *PDE6B*), four were classified as likely benign (*ABCA4*, *CACNA1F*, *EYS*, and *USH2A*), one as likely pathogenic (*EYS*), and one as pathogenic (*LRAT*) according to American College of Medical Genetics and Genomics (ACMG) guidelines[46] (Table 1, **Supplemental Digital Content 2**). The likely pathogenic *EYS* variant p.(Trp558*) was present heterozygously in two siblings (K1, K2) who originated from the genetic isolate. The pathogenic *LRAT* variant was previously described by Littink et al,[47] in the same genetic isolate, and leads to a frameshift. This variant was found heterozygously in a single patient (O3) who also stemmed from this isolate.

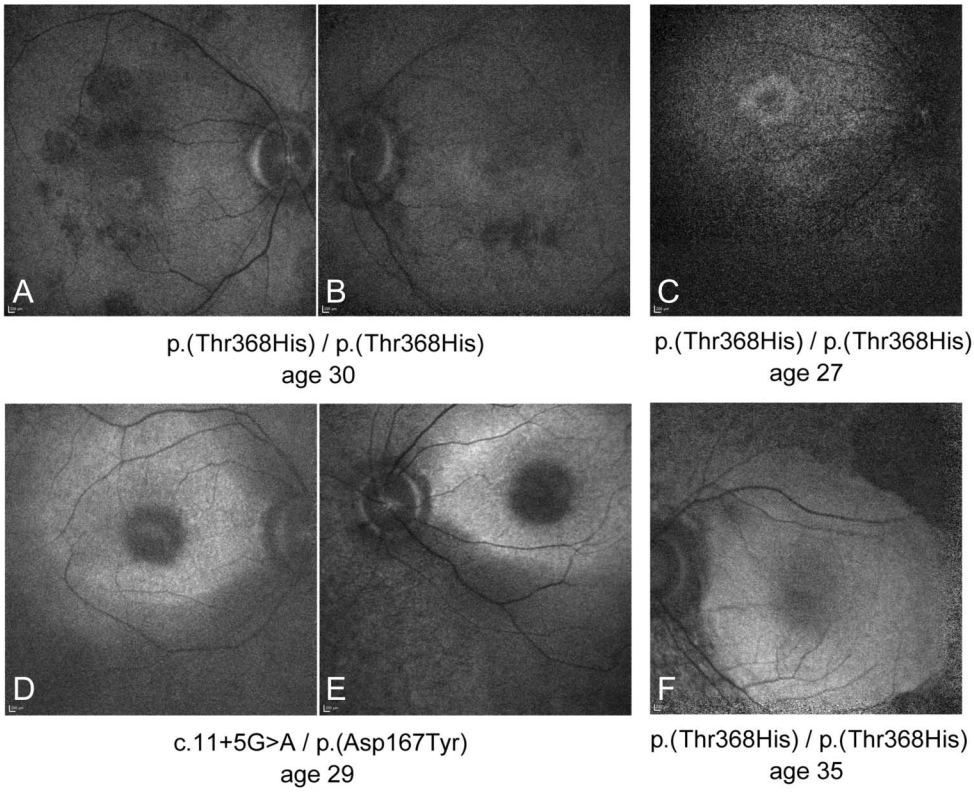

Fig. 5. Fundus autofluorescence in patients with RPE65-mediated IRDs. Fundus autofluorescence imaging in patient O3 (**A** and **B**) and patient O2 (**C**) shows a small hyperautofluorescent ring around the fovea. In patient AA1 (**D** and **E**) and patient V2 (**F**), the macula appears partially hyperautofluorescent.

Genotype–Phenotype Correlation

There was no significant difference in course of disease in subjects with different combinations of variants. We plotted all BCVA measurements against age for all patients in Figure 6. Patients homozygous for the founder variant p.(Tyr368His) did not appear to perform significantly better or worse than subjects with other genotypes, and their visual performance was not clustered but spread over the whole range of BCVA values at different ages. The interfamilial and intrafamilial variability in visual function was high, even in patients with an identical *RPE65* genotype. We compared visual function of siblings from two families (Figure 8), one homozygous for c.11+5 G>A (Family AB) and the second homozygous for p.(Thr368His) (Family O) within the same age range and observed a large heterogeneity in visual function. Patient AB2 showed atrophy of the macula, at age 32, while his brother (AB1) was still able to read print at age 30. In Family O, the eldest brother (O3) had a better visual function than his younger siblings (O1-2) from childhood onward.

Discussion

In this study, we assessed the natural course of the disease of *RPE65*-mediated IRDs by analyzing longitudinal data from a large cohort of subjects (n = 45) with biallelic pathogenic *RPE65* variants, of which 28 subjects stem from a genetic isolate. This genetic homogeneity of a large part of the study population gave us the unique opportunity to look for genotype–phenotype correlations. Our study shows that visual function varies widely early in life but deteriorates inevitably toward blindness. The percentage of patients meeting the WHO criteria for blindness increases with age and reaches 100% after the age of 40 years. We did not observe a correlation between the *RPE65*-genotype and the phenotype in this study, and visual function varied significantly even between siblings. Additional screening of 108 IRD-associated genes in 35 patients revealed a single pathogenic *LRAT* variant in one patient and a novel likely pathogenic *EYS* variant in two siblings, in addition to the previously detected *RPE65* variants. Hence, there were no patients with double hit IRDs.

RPE65-associated IRD was diagnosed within the first year(s) of life in patients born in the Netherlands. In the genetic isolate, the awareness toward *RPE65*-mediated IRDs was high, as many inhabitants had affected family members, and the disease prevalence was markedly elevated. Hallmarks of *RPE65*-mediated IRD are severe night blindness and photoattraction from infancy caused by the rod–cone dystrophy.[18,48]

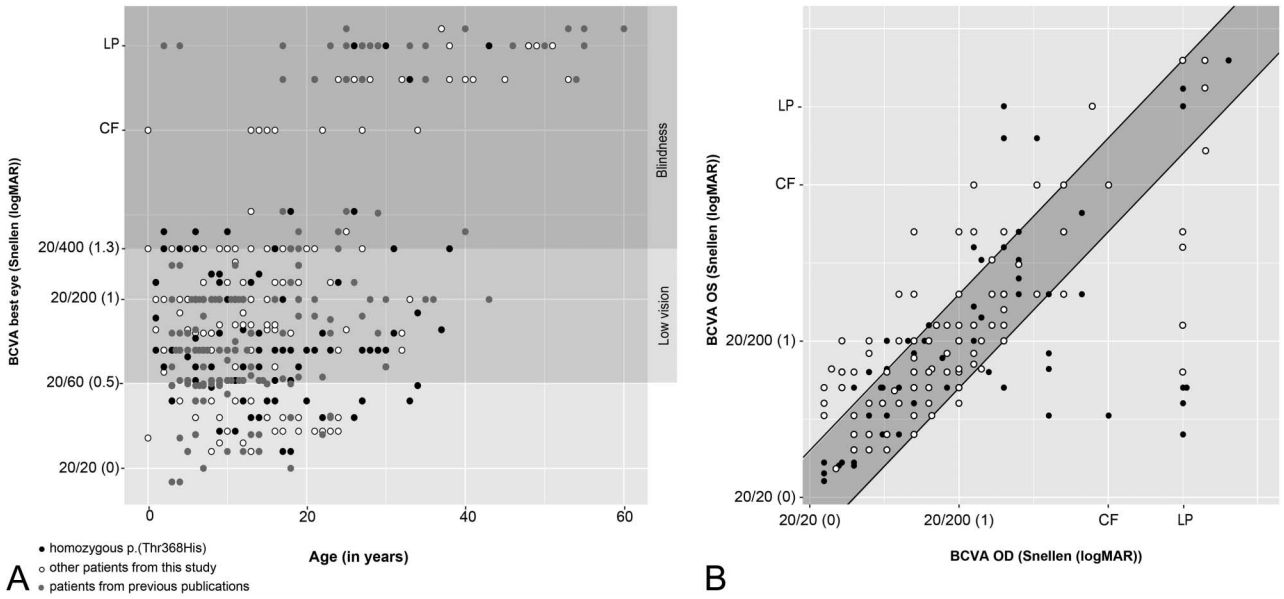

Fig. 6. Visual acuity as a function of time and comparison of visual acuity measurements between both eyes measured in a single visit. Measurements of subjects homozygous for the p.(Thr368His) founder mutation are represented by black dots, measurements in subjects with other genotypes are represented by white dots, and subjects from previous publications[8,16–37] are represented by gray dots. **A.** Scatterplot of BCVA measurements of the best eye in dependence of age. WHO criteria for blindness (BCVA $<$ 20/400; dark gray) and low vision (20/60 $>$ BCVA $\geq$ 20/400; light gray) are marked. **B.** Scatterplot of VA measurements of the left eye in dependence of the right eye. The gray-filled banner represents the test–retest variability of 4 lines (0.3 LogMAR), which corresponds to 15 ETRDS letters. Fifty-six measurements of 19 patients were outside the range of 4 lines (0.3 LogMAR) difference: In 8 patients, the difference was measured on one occasion, and in 11 patients, the difference was measured on 2 or more occasions. OD, right eye; OS, left eye.

Nystagmus can be observed but is not inherent to *RPE65*-mediated IRD and was not directly correlated to visual acuity in our cohort. In the Netherlands, genetic testing is routinely performed in infants, but also in older patients newly diagnosed with IRDs. Up until now, we have not come across patients with late-onset *RPE65*-mediated IRDs in our clinics.

Infants with *RPE65*-associated IRDs had subtle funduscopic changes (hypopigmentation, RPE alterations, and narrow blood vessels). Signs of retinal degeneration, such as bone spicule pigmentations, and atrophy of the RPE, only became apparent in the second decade of life. Thirteen patients developed perifoveal atrophy, from as early as the age of 17 years, which advanced toward the fovea and proved detrimental for visual performance.

Spectral domain OCTs were selected based on their quality and suitability for manual segmentation and compared with OCTs of controls. It was challenging to make good-quality scans, in patients with poor visual function and severe nystagmus; as a consequence, our results may lack the severe end of the spectrum. We confirm that retinal lamellar architecture in the macula was mostly preserved in children.[15,20,49,50] One child showed signs of retinal degeneration on OCT at an early age (Figure 4D). Children with preserved lamellar structure did not always have good visual acuity, and the EZ appeared less intense than in controls. This may be due to the RPE65 dysfunction. In adults, however, clearly distinguishable retinal layers in the fovea (Figure 4, E–H) were associated with visual acuity that was remarkably better than in patients with pronounced atrophy. The ONL and outer retinal layer were significantly thinner in patients in all age categories compared with controls (Figure 3). Outer nuclear layer thickness is often used as a marker for retinal remodeling in different types of IRDs.[51–53]

Fundus autofluorescence is based on the excitation of fluorophores in lipofuscin, which is a byproduct of the visual cycle. RPE65 is a key enzyme of the visual cycle as it transforms all-trans-retinyl esters into 11-cis retinol; thus, patients with *RPE65*-associated IRDs might not be able to form lipofuscin at all. Previous studies showed absent or very low autofluorescence levels in patients[17,54] and mice with *RPE65*-mediated IRDs.[43] Hypomorphic *RPE65* mutations were associated with residual protein activity in in vitro studies. As lipofuscin levels were proposed as a surrogate for RPE65 activity, there should be enhanced autofluorescence present in patients with hypomorphic mutations,[26] but we did not have any patients with previously tested hypomorphic mutations (Table 3). Fundus autofluorescence with 488 nm was absent in our patients. Even generating cSLO FAF images with

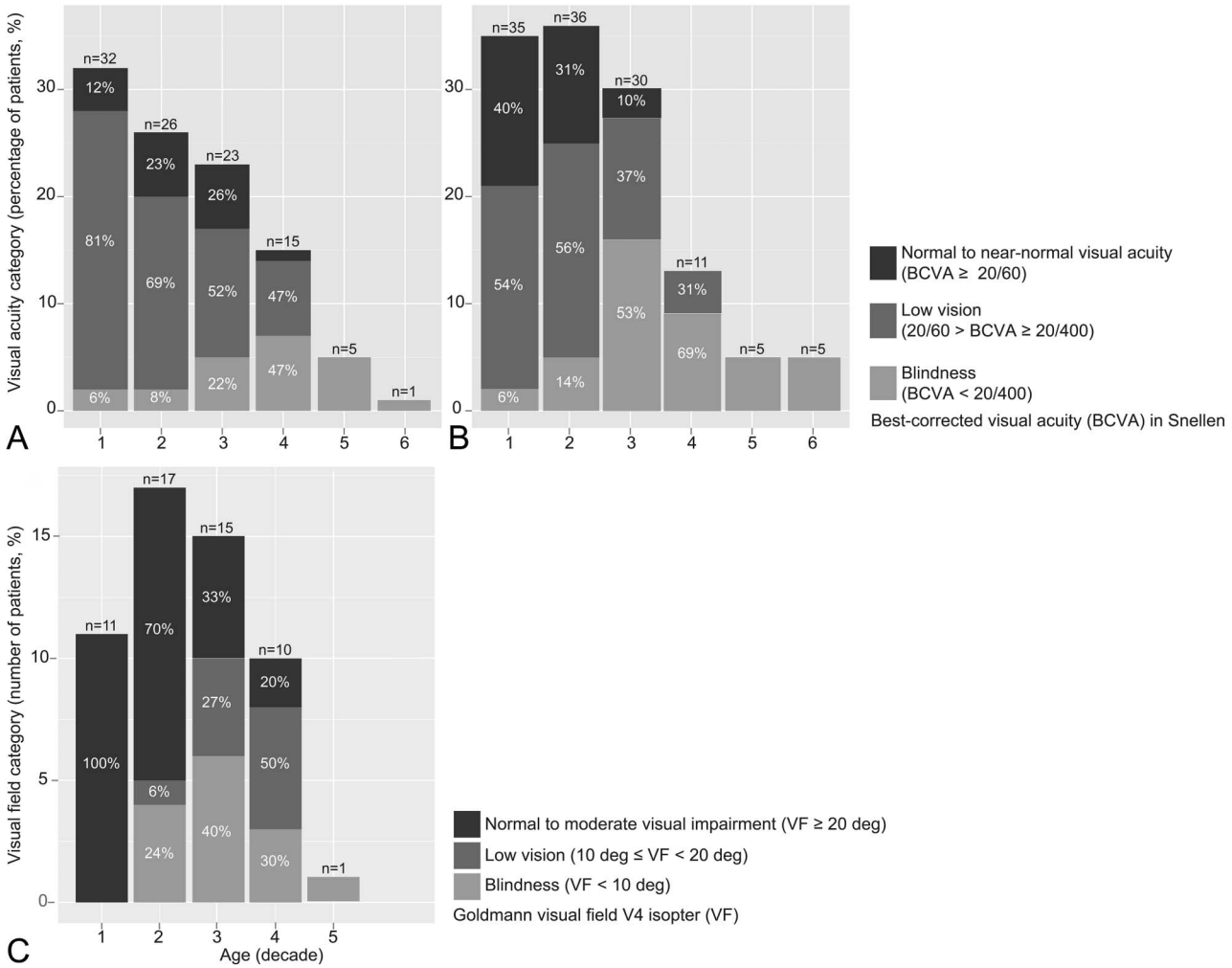

Fig. 7. Course of visual acuity and VF as a function of time. Stacked bar-charts showing the distribution of BCVA per age category (**A**) in our study cohort and (**B**) in pooled data from previously published studies,[8,16–37] only data before treatment were included for analysis. When multiple measurements were available for a patient within one decade, the mean was taken. The percentage of patients meeting the criteria for legal blindness increases with age and reaches 100% over the age of 40 years in both populations. **C** shows the distribution of VF per age category. There were no published data available for comparison. Low vision and blindness criteria were in accordance with the World Health Organization.

inadequate sensitivity settings proved difficult in this patient group because of nystagmus, poor fixation, and patients' discomfort. Overall autofluorescence in our cohort was reduced compared with controls. In two patients, of which one carried at least one nonhypomorphic variant (Figure 5, D and E) and a second patient with a homozygous nonhypomorphic variant (Figure 5F), the macula appeared hyperautofluorescent compared with the midperiphery. Two patients with nonhypomorphic mutations had a hyperautofluorescent ring around the fovea (Figure 5, A and C) as typically observed in patients with rod–cone dystrophies such as retinitis pigmentosa.[55] This ring has also been observed in hypomorphic *RPE65* mutations by Hull et al,[26] but judging from the aspect of the optic nerve, these images seemed also to be acquired with suboptimal exposure settings. Consequently, we cannot certify that the hyperautofluorescent signal in our subjects was produced by lipofuscin, and care must be taken with interpretation.

Loss of isomerization activity typically leads to overaccumulation of all-trans-retinyl esters. Animal models show that white dots are accumulations of retinyl esters within lipid droplets.[5,56,57] They are often observed in patients with retinol dehydrogenase 5 (*RDH5)*-, retinaldehyde binding protein 1 (*RLBP1)*-, and lecithin retinol acyltransferase (*LRAT)*-associated fundus albipunctatus, fundus albipunctatus associated with cone–rod disease, and retinitis punctata albescens. All three genes are part of the vitamin A cycle. We have observed white dots in one patient with severe visual impairment at a young age and three patients with moderate visual impairment. The presence of white dots has previously been associated with

Table 3. *RPE65* Variants in this Study, Their Isomerase Activity, and In Silico Functional Analyses

DNA Variation	Protein/Splicing Variation	dbSNP id	Isomerase Activity	SIFT	PolyPhen2	Grantham Score	CADD Score	gnomAD Frequency	Allele Frequency in This Study
c.11+5 G>A	p.?	rs61751276	NA					0.00009	10 (11%)
c.138delG	p.(Pro47Glnfs*47)	NA	NA					0	4 (4%)
c.208T>G	p.(Phe70Val)	NA	NA	0.22	1	50	27.00	0	1 (1%)
c.271C>T	p.(Arg91Trp)	rs61752871	5.08% of WT (±0.538 SD)[44]	0.01	0.999	101	17.12	0.00005	9 (10%)
c.361delT	p.(Serf121 fs*)	NA	NA					0	1 (1%)
c.499 G>T	p.(Asp167Tyr)	rs61752883	NA	0.07	1	160	18.15	0.00001	1 (1%)
c.715T>G	p.(Tyr239Asp)	rs61752896	4.59% of WT (±0.414 SD)[44]	0	1	160	21.40	0.00001	7 (8%)
c.859 G>T	p.(Val287Phe)	rs281865289	NA	0.02	0.989	50	18.77	0	2 (2%)
c.989 G>A	p.(Cys330Thr)	rs61752908	NA	0.72	0.998	184	17.17	0.000005	2 (2%)
c.991-993dup	p.(Trp331dup)	NA	NA					0	1 (1%)
c.1102T>C	p.(Tyr368His)	rs62653011	<3% of WT[58]	0	1	83	24.40	0.00007	49 (54%)
c.1067dup	p.(Asn356Lysfs*9)	rs766074572	NA					0.00003	2 (2%)
c.1543C>T	p.(Arg515Trp)	rs121917745	NA	0	1	101	18.70	0.00002	1 (1%)

CADD, combined annotation dependent depletion; gnomAD, genome aggregation database; NA, not available; PolyPhen2, polymorphism phenotyping v2; SIFT, sorting intolerant from tolerant; WT, wild type.

both mild[23,26] and severe[24] disease phenotypes. It might prove difficult to identify white dots in patients with nystagmus or a blond aspect of the fundus; furthermore, these dots disappear over time, which might have led to an underestimation of its prevalence in our cohort. Drüsen-like deposits are a common feature in patients with IRDs and might resemble white dots strongly. We are reluctant to associate white dots with a more severe disease phenotype because we observed them in four cases only.

Visual acuity in the first decade of life ranged from 20/20 to counting fingers at 1 m. A larger proportion of children were visually impaired in our cohort when compared with pooled visual acuity data from previous publications[8,16–37] (Figure 7, A and B). Most subjects were able to learn to read print as a child, and visual acuity remained stable until adolescence. We did not measure a transient improvement in visual acuity in childhood, as suggested by Perrault et al.[48] Five patients had one amblyopic eye with a difference in visual acuity of more than four lines (0.3 LogMAR). In the majority, visual acuity was symmetric between both eyes. Over the age of 40 years, all patients were blind according to WHO criteria for visual acuity (Figure 7, A and B) because of progressive retinal degeneration. These findings are consistent with a recent publication by Chung et al[58]; visual acuity in the first three decades was slightly better in our cohort. This may be due to a difference in approach of analyzing visual function data, as we looked at visual acuity of the best- and worst-performing eye, while Chung et al made a distinction between the right and left eye. We were not able to compare VF results as we used a qualitative, rather than a quantitative method.

We observed considerable variability in visual function between patients, even in subjects carrying identical *RPE65* variants. In 19 subjects who were homozygous for the p.(Thr368His) variant, the severity of disease in the first four decades of life differed substantially (Figures 6 and 7). Even among siblings, who share more genetic material (~50%) and were exposed to similar environmental factors during childhood, the course of disease varied widely (Figures 6A and 8). The p.(Thr368His) variant was previously described as a nonhypomorphic variant, functional in vitro studies revealed it had only <3% isomerization activity compared with wild type.[59] Despite carrying a homozygous mutation that severely diminishes isomerization activity (i.e., nonhypomorphic residues), some subjects had a good visual function at an early age up to young adulthood. This mild phenotype was previously described[21,26] in four patients carrying missense mutations, resulting in hypomorphic residues, but not in patients with nonhypomorphic residues.

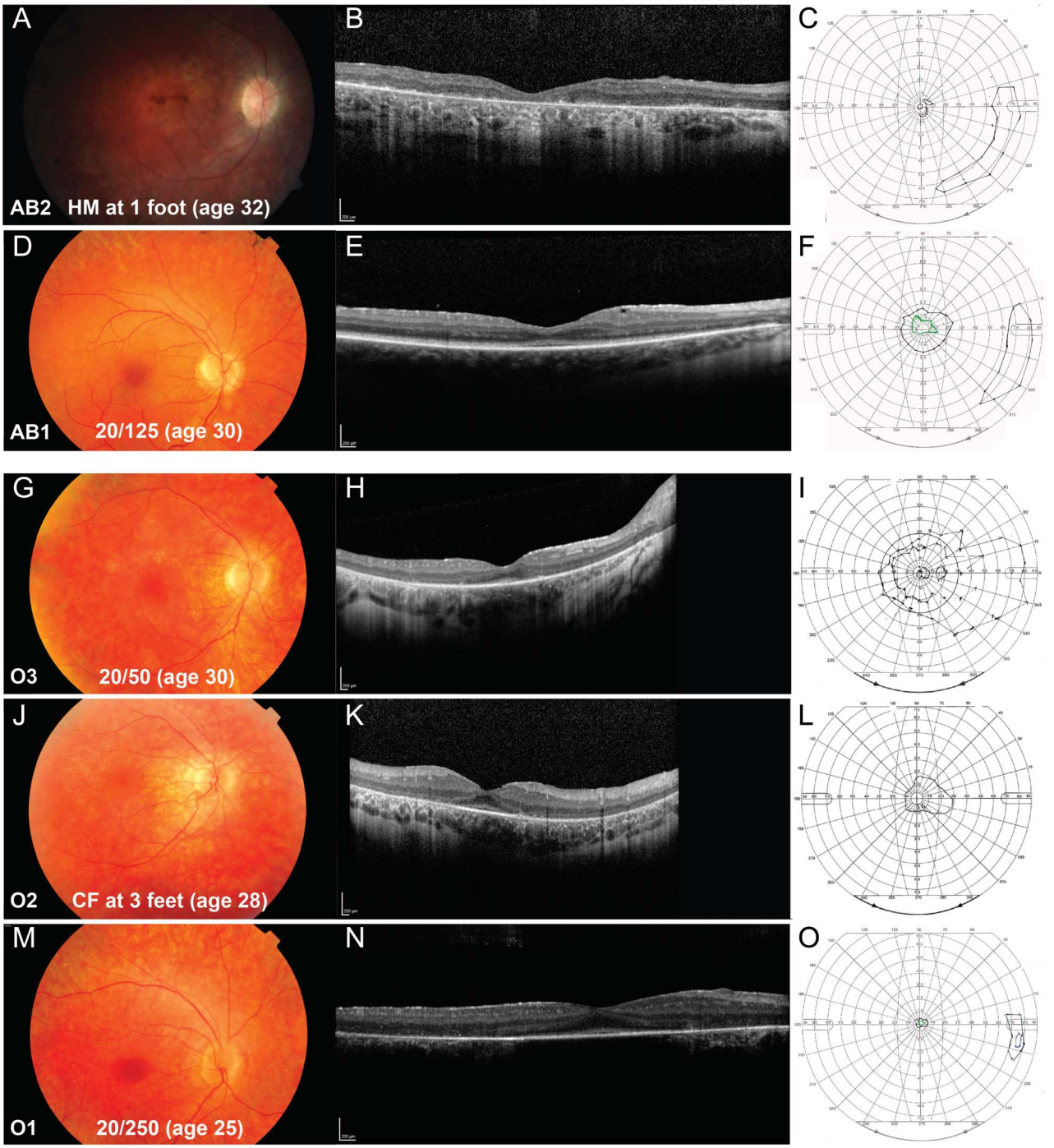

Fig. 8. Comparison of fundus images, BCVA measurements, infrared (IR) images, SD-OCT scans, and Goldmann VFs of siblings of two families within the same age range. In family AB, the eldest brother (AB2) had markedly worse BCVA and smaller VF than his younger brother (AB1). Fundus imaging, IR, and SD-OCT demonstrate (**A** and **B**) (AB1) central atrophy of the outer retina: The ELM is absent, and ellipsoid zone and interdigitation zone are disrupted. His brother (**D** and **E**) (AB2) has a distorted inner retinal architecture and no recognizable ELM. The ellipsoid zone and interdigitation zone appear intact in the macula. Both siblings have a peripheral island temporally; the oldest sibling (**C**) has a small remaining central VF with a radius below 5° measured with the V4 target, and the youngest sibling (**F**) has a central VF of 15° radius measured with the V4 target and 10° with the III4 target. In family O, the eldest sibling (O3) has a markedly better BCVA and larger VF (**I, L, O**) than his siblings (O1, O2) which is not clearly reflected in SD-OCT imaging. He has (**G, H**) parafoveal atrophy of the outer retina with central sparing of the ellipsoid and interdigitation zone, outer retinal tubulation, and there appear to be some remnants of the ELM. His sister (**J, K**) (O2) has similar parafoveal atrophy of the outer segments with sparing of the ellipsoid and interdigitation zone. The youngest sibling (**M, N**) (O1) has parafoveal atrophy of the outer segments; it is not possible to distinguish the remaining outer retinal layers in the center because of the quality of the scan. The VF of the oldest sibling (**I**) (O3) is relatively well preserved and reaches 60° temporally and 30° nasally with the V4 target, and the VF of his younger sister (**L**) (O2) is markedly smaller and barely reaches 30° temporally and 10° nasally with the V4 target. The youngest sibling (**O**) (O1) has a very small tunnel vision with a radius less than 5° and a small temporal peripheral island.

So, the *RPE65* genotype appeared to have no prognostic value for the visual performance and disease progression in our cohort. Explanations for clinical variation may be sought in reduced penetrance, differential allelic expression, copy number variation, or modifying genetic variants in cis or trans.[60] To zoom in on the latter, we screened 108 IRD-associated genes for pathogenic variants that may influence the phenotype. Visual cycle genes were of special interest, such as *ABCA4*, *LRAT*, and *RDH12*. In addition, we wanted to rule out a double hit because there was a high prevalence of consanguinity in our cohort, and there were patients with *FAM161A*-, *LRAT*-, and *USH2A*-associated IRDs in the genetic isolate.

Molecular Inversion Probe analysis of 108 IRD-associated genes confirmed all previously sequenced *RPE65* variants. We detected a heterozygous frameshift variant in *LRAT* in one patient, and a heterozygous nonsense *EYS* variant in two siblings, all three stemming from the genetic isolate. The *LRAT* variant was described in four patients with retinitis punctata albescens, originating from the same genetic isolate.[47] The *LRAT* gene is involved in the visual cycle; it catalyzes the esterification of all-trans-retinol into all-trans-retinyl ester, which is later transformed by RPE65 into 11-cis-retinol. Whether this frameshift *LRAT* variant could have a modifying effect on the visual cycle, and thus on the retinal dysfunction in patients with *RPE65*-associated IRDs, remains to be identified. Patient O3, who carried this variant, had a relatively mild phenotype, which does not suggest a very deleterious effect of the additional *LRAT* variant. The novel *EYS* variant found in two siblings (K1, K2) induces a premature stop codon and is predicted to be pathogenic. *EYS* is not part of the visual cycle but is responsible for the structural integrity of photoreceptor cells. One in four to five (20%–25%) individuals from the general world population was estimated to be a carrier of a mutation in any IRD gene.[61] In our study, 3 of 35 (9%) individuals carried a pathogenic variant in another IRD gene, in addition to the biallelic *RPE65* variants.

Up to now, gene therapy has improved patients' mobility in dim light, enlarged VF, and sometimes improved visual acuity, all to varying degrees.[8,10–12,42,62–65] Serious adverse events were rare (e.g., endophthalmitis, macular hole, and retinal thinning), but treatment proved not to be without risk, and the degenerative process was not slowed by the intervention. Preintervention visual function in younger patients was often better than in adults at baseline; therefore, it was hard to assess age-dependent effects of treatment. However, we advocate to initiate treatment as early as possible, to target more viable photoreceptor cells, and to stay ahead of the degenerative component.[8,10–12] There was no consensus on whether the fovea needs to be included within the subretinal vector bleb, but if treated, it was recommended to keep the injected volume small to minimalize the foveal dehiscence.[8,12] Atrophy of the fovea might make it difficult to spread the vector bleb after injection; second, the gain in visual acuity might be limited because there are little viable photoreceptors left that benefit from treatment. High myopia and the associated retinal thinning were considered a contraindication for foveal treatment.[11]

Over the past decades, we have closely followed a cohort of 45 patients with *RPE65*-mediated IRDs to gain insight into the course of disease and assess genotypic and phenotypic heterogeneity. The most important limitation of this study is inherent to its retrospective design. Data were gathered over five decades, and therefore, not all measurements were available for all patients. In our clinic, SD-OCT imaging became available in 2008, followed by FAF imaging. In patients with *RPE65*-mediated IRDs, the quality of these techniques is often limited by the inability of central fixation because of nystagmus and photoaversion. For future studies, we suggest the combination of multimodal imaging with fundus-controlled perimetry to better correlate visual function with retinal structure. All patients developed symptoms within the first year of life. Most children had retinal abnormalities at first examination. Visual function early in life varied and remained stable until adolescence, but deteriorated inevitably toward blindness after the age of 40 years. Thirteen patients developed profound atrophy of the macula during follow-up; this process started in the perifoveal region and reached the fovea over the course of years. We did not perceive a prognostic value of the *RPE65* genotype in our cohort. Three of 35 (9%) patients tested with MIP analysis carried an additional pathogenic variant in another IRD-associated gene (*LRAT* and *EYS*). No patients could be diagnosed with a double hit IRD.

Key words: gene therapy, genetics, inherited retinal degeneration, Leber congenital amaurosis, optical coherence tomography, RPE65, retinitis pigmentosa, visual field.

References

1. Kumaran N, Moore AT, Weleber RG, Michaelides M. Leber congenital amaurosis/early-onset severe retinal dystrophy: clinical features, molecular genetics and therapeutic interventions. Br J Ophthalmol 2017;101:1147–1154.
2. Leber T. Ueber retinitis pigmentosa und angeborene amaurose. Graefes Arch Clin Exp Ophthalmol 1869;15:1–25.
3. Leber T, Netzhaut DI, Saemish T. Graefe Handbuch der gesamten Augenheilkunde. 2nd ed. Leipzig, Germany: W. Engelman; 1916.

4. Koenekoop RK. An overview of Leber congenital amaurosis: a model to understand human retinal development. Surv Ophthalmol 2004;49:379–398.
5. Redmond TM, Yu S, Lee E, et al. Rpe65 is necessary for production of 11-cis-vitamin A in the retinal visual cycle. Nat Genet 1998;20:344–351.
6. Muniz A, Villazana-Espinoza ET, Hatch AL, et al. A novel cone visual cycle in the cone-dominated retina. Exp Eye Res 2007;85:175–184.
7. Koenekoop RK, Sui R, Sallum J, et al. Oral 9-cis retinoid for childhood blindness due to Leber congenital amaurosis caused by RPE65 or LRAT mutations: an open-label phase 1b trial. Lancet 2014;384:1513–1520.
8. Bainbridge JW, Mehat MS, Sundaram V, et al. Long-term effect of gene therapy on Leber's congenital amaurosis. N Engl J Med 2015;372:1887–1897.
9. Jacobson SG, Cideciyan AV, Roman AJ, et al. Improvement and decline in vision with gene therapy in childhood blindness. N Engl J Med 2015;372:1920–1926.
10. Weleber RG, Pennesi ME, Wilson DJ, et al. Results at 2 Years after gene therapy for RPE65-deficient leber congenital amaurosis and severe early-childhood-onset retinal dystrophy. Ophthalmology 2016;123:1606–1620.
11. Bennett J, Wellman J, Marshall KA, et al. Safety and durability of effect of contralateral-eye administration of AAV2 gene therapy in patients with childhood-onset blindness caused by RPE65 mutations: a follow-on phase 1 trial. Lancet 2016;388:661–672.
12. Maguire AM, High KA, Auricchio A, et al. Age-dependent effects of RPE65 gene therapy for Leber's congenital amaurosis: a phase 1 dose-escalation trial. Lancet 2009;374:1597–1605.
13. Krishnamoorthy V, Cherukuri P, Poria D, et al. Retinal remodeling: concerns, emerging remedies and future prospects. Front Cell Neurosci 2016;10:38.
14. Porto FB, Perrault I, Hicks D, et al. Prenatal human ocular degeneration occurs in Leber's congenital amaurosis (LCA2). J Gene Med 2002;4:390–396.
15. Jacobson SG, Cideciyan AV, Aleman TS, et al. Photoreceptor layer topography in children with leber congenital amaurosis caused by RPE65 mutations. Invest Ophthalmol Vis Sci 2008;49:4573–4577.
16. Felius J, Thompson DA, Khan NW, et al. Clinical course and visual function in a family with mutations in the RPE65 gene. Arch Ophthalmol 2002;120:55–61.
17. Lorenz B, Wabbels B, Wegscheider E, et al. Lack of fundus autofluorescence to 488 nanometers from childhood on in patients with early-onset severe retinal dystrophy associated with mutations in RPE65. Ophthalmology 2004;111:1585–1594.
18. Lorenz B, Gyürüs P, Preising M, et al. Early-onset severe rod-cone dystrophy in young children with RPE65 mutations. Invest Ophthalmol Vis Sci 2000;41:2735–2742.
19. Paunescu K, Wabbels B, Preising MN, Lorenz B. Longitudinal and cross-sectional study of patients with early-onset severe retinal dystrophy associated with RPE65 mutations. Graefes Arch Clin Exp Ophthalmol 2005;243:417–426.
20. Simonelli F, Ziviello C, Testa F, et al. Clinical and molecular genetics of Leber's congenital amaurosis: a multicenter study of Italian patients. Invest Ophthalmol Vis Sci 2007;48:4284–4290.
21. Lorenz B, Poliakov E, Schambeck M, et al. A comprehensive clinical and biochemical functional study of a novel RPE65 hypomorphic mutation. Invest Ophthalmol Vis Sci 2008;49:5235–5242.
22. Jacobson SG, Aleman TS, Cideciyan AV, et al. Defining the residual vision in leber congenital amaurosis caused by RPE65 mutations. Invest Ophthalmol Vis Sci 2009;50:2368–2375.
23. Schatz P, Preising M, Lorenz B, et al. Fundus albipunctatus associated with compound heterozygous mutations in RPE65. Ophthalmology 2011;118:888–894.
24. Weleber RG, Michaelides M, Trzupek KM, et al. The phenotype of severe early childhood onset retinal dystrophy (SECORD) from mutation of RPE65 and differentiation from leber congenital amaurosis. Invest Ophthalmol Vis Sci 2011;52:292–302.
25. Scholl HP, Moore AT, Koenekoop RK, et al. Safety and proof-of-concept study of oral QLT091001 in retinitis pigmentosa due to inherited deficiencies of retinal pigment epithelial 65 protein (RPE65) or lecithin:retinol acyltransferase (LRAT). PLoS One 2015;10:e0143846.
26. Hull S, Holder GE, Robson AG, et al. Preserved visual function in retinal dystrophy due to hypomorphic RPE65 mutations. Br J Ophthalmol 2016;100:1499–1505.
27. Sitorus RS, Lorenz B, Preising MN. Analysis of three genes in Leber congenital amaurosis in Indonesian patients. Vision Res 2003;43:3087–3093.
28. Gu SM, Thompson DA, Srikumari CR, et al. Mutations in RPE65 cause autosomal recessive childhood-onset severe retinal dystrophy. Nat Genet 1997;17:194–197.
29. Al-Khayer K, Hagstrom S, Pauer G, et al. Thirty-year follow-up of a patient with leber congenital amaurosis and novel RPE65 mutations. Am J Ophthalmol 2004;137:375–377.
30. Poehner WJ, Fossarello M, Rapoport AL, et al. A homozygous deletion in RPE65 in a small Sardinian family with autosomal recessive retinal dystrophy. Mol Vis 2000;6:192–198.
31. Hamel CP, Griffoin JM, Lasquellec L, et al. Retinal dystrophies caused by mutations in RPE65: assessment of visual functions. Br J Ophthalmol 2001;85:424–427.
32. Biswas P, Duncan JL, Maranhao B, et al. Genetic analysis of 10 pedigrees with inherited retinal degeneration by exome sequencing and phenotype-genotype association. Physiol Genomics 2017;49:216–229.
33. Srilekha S, Arokiasamy T, Srikrupa NN, et al. Homozygosity mapping in leber congenital amaurosis and autosomal recessive retinitis pigmentosa in South Indian families. PLoS One 2015;10:e0131679.
34. Verma A, Perumalsamy V, Shetty S, et al. Mutational screening of LCA genes emphasizing RPE65 in South Indian cohort of patients. PLoS One 2013;8:e73172.
35. Chen Y, Zhang Q, Shen T, et al. Comprehensive mutation analysis by whole-exome sequencing in 41 Chinese families with Leber congenital amaurosis. Invest Ophthalmol Vis Sci 2013;54:4351–4357.
36. Xu F, Dong Q, Liu L, et al. Novel RPE65 mutations associated with Leber congenital amaurosis in Chinese patients. Mol Vis 2012;18:744–750.
37. Singh HP, Jalali S, Narayanan R, Kannabiran C. Genetic analysis of Indian families with autosomal recessive retinitis pigmentosa by homozygosity screening. Invest Ophthalmol Vis Sci 2009;50:4065–4071.
38. Yzer S, van den Born LI, Schuil J, et al. A Tyr368His RPE65 founder mutation is associated with variable expression and progression of early onset retinal dystrophy in 10 families of a genetically isolated population. J Med Genet 2003;40:709–713.
39. van Huet RA, Oomen CJ, Plomp AS, et al. The RD5000 database: facilitating clinical, genetic, and therapeutic studies on

inherited retinal diseases. Invest Ophthalmol Vis Sci 2014;55: 7355–7360.
40. Hyvärinen L, Näsänen R, Laurinen P. New visual acuity test for pre-school children. Acta Ophthalmol (Copenh) 1980;58: 507–511.
41. Lange C, Feltgen N, Junker B, et al. Resolving the clinical acuity categories hand motion and counting fingers using the Freiburg Visual Acuity Test (FrACT). Graefes Arch Clin Exp Ophthalmol 2009;247:137–142.
42. Russell S, Bennett J, Wellman JA, et al. Efficacy and safety of voretigene neparvovec (AAV2-hRPE65v2) in patients with RPE65-mediated inherited retinal dystrophy: a randomised, controlled, open-label, phase 3 trial. Lancet 2017;390:849–860.
43. Katz ML, Redmond TM. Effect of Rpe65 knockout on accumulation of lipofuscin fluorophores in the retinal pigment epithelium. Invest Ophthalmol Vis Sci 2001;42:3023–3030.
44. Philp AR, Jin M, Li S, et al. Predicting the pathogenicity of RPE65 mutations. Hum Mutat 2009;30:1183–1188.
45. Hofman A, van Duijn CM, Franco OH, et al. The Rotterdam Study: 2012 objectives and design update. Eur J Epidemiol 2011;26:657–686.
46. Richards S, Aziz N, Bale S, et al. Standards and guidelines for the interpretation of sequence variants: a joint consensus recommendation of the American College of Medical Genetics and Genomics and the Association for Molecular Pathology. Genet Med 2015;17:405–424.
47. Littink KW, van Genderen MM, van Schooneveld MJ, et al. A homozygous frameshift mutation in LRAT causes retinitis punctata albescens. Ophthalmology 2012;119:1899–1906.
48. Perrault I, Rozet JM, Ghazi I, et al. Different functional outcome of RetGC1 and RPE65 gene mutations in Leber congenital amaurosis. Am J Hum Genet 1999;64:1225–1228.
49. Jacobson SG, Cideciyan AV, Aleman TS, et al. RDH12 and RPE65, visual cycle genes causing leber congenital amaurosis, differ in disease expression. Invest Ophthalmol Vis Sci 2007; 48:332–338.
50. Pasadhika S, Fishman GA, Stone EM, et al. Differential macular morphology in patients with RPE65-, CEP290-, GUCY2D-, and AIPL1-related Leber congenital amaurosis. Invest Ophthalmol Vis Sci 2010;51:2608–2614.
51. McGuigan DB, Heon E, Cideciyan AV, et al. EYS mutations causing autosomal recessive retinitis pigmentosa: changes of retinal structure and function with disease progression. Genes (Basel) 2017;8.
52. Jones BW, Pfeiffer RL, Ferrell WD, et al. Retinal remodeling in human retinitis pigmentosa. Exp Eye Res 2016;150:149–165.
53. Aleman TS, Cideciyan AV, Sumaroka A, et al. Inner retinal abnormalities in X-linked retinitis pigmentosa with RPGR mutations. Invest Ophthalmol Vis Sci 2007;48:4759–4765.
54. Wabbels B, Demmler A, Paunescu K, et al. Fundus autofluorescence in children and teenagers with hereditary retinal diseases. Graefes Arch Clin Exp Ophthalmol 2006;244:36–45.
55. Robson AG, El-Amir A, Bailey C, et al. Pattern ERG correlates of abnormal fundus autofluorescence in patients with retinitis pigmentosa and normal visual acuity. Invest Ophthalmol Vis Sci 2003;44:3544–3550.
56. Maeda A, Maeda T, Imanishi Y, et al. Aberrant metabolites in mouse models of congenital blinding diseases: formation and storage of retinyl esters. Biochemistry 2006;45:4210–4219.
57. Travis GH, Golczak M, Moise AR, Palczewski K. Diseases caused by defects in the visual cycle: retinoids as potential therapeutic agents. Annu Rev Pharmacol Toxicol 2007;47:469–512.
58. Chung DC, Bertelsen M, Lorenz B, et al. The natural history of inherited retinal dystrophy due to biallelic mutations in the RPE65 gene. Am J Ophthalmol 2019;199:58–70.
59. Redmond TM, Poliakov E, Yu S, et al. Mutation of key residues of RPE65 abolishes its enzymatic role as isomerohydrolase in the visual cycle. Proc Natl Acad Sci USA 2005;102: 13658–13663.
60. Cooper DN, Krawczak M, Polychronakos C, et al. Where genotype is not predictive of phenotype: towards an understanding of the molecular basis of reduced penetrance in human inherited disease. Hum Genet 2013;132:1077–1130.
61. Nishiguchi KM, Rivolta C. Genes associated with retinitis pigmentosa and allied diseases are frequently mutated in the general population. PLoS One 2012;7:e41902.
62. Simonelli F, Maguire AM, Testa F, et al. Gene therapy for Leber's congenital amaurosis is safe and effective through 1.5 years after vector administration. Mol Ther 2010;18:643–650.
63. Maguire AM, Simonelli F, Pierce EA, et al. Safety and efficacy of gene transfer for Leber's congenital amaurosis. N Engl J Med 2008;358:2240–2248.
64. Bennett J, Ashtari M, Wellman J, et al. AAV2 gene therapy readministration in three adults with congenital blindness. Sci Transl Med 2012;4:120ra15.
65. Bainbridge JW, Smith AJ, Barker SS, et al. Effect of gene therapy on visual function in Leber's congenital amaurosis. N Engl J Med 2008;358:2231–2239.